

In absence of feedback, the above equation yields the complete statistics of electrons (current, noise, skewness etc.) that have tunneled across the SET [4]. At small SET bias, the QPC does not resolve to which of the attached leads a tunneling process has happened. Therefore, simplest feedback operations can only be conditioned on whether the SET is empty or filled (scheme I) or whether an electron has jumped into or out of the SET (schemes IIa/b). Such control operations may easily be included in the numerical solution of Eq. (2) via an associated stochastic Schrödinger equation [5]. For analytic results however, it is more favorable to derive an effective Liouvillian under feedback, which enables one to systematically study the effects of feedback on the statistics.

In our simplest *scheme I*, we only apply two different Liouvillians – conditioned on whether the SET is empty ($\mathcal{L}_E(\chi_L, \chi_R) \equiv \sum_\alpha \Gamma_\alpha e^{\delta_\alpha^E} \mathcal{F}_\alpha(\chi_\alpha)$) or filled ($\mathcal{L}_F(\chi_L, \chi_R) \equiv \sum_\alpha \Gamma_\alpha e^{\delta_\alpha^F} \mathcal{F}_\alpha(\chi_\alpha)$), where the dimensionless feedback parameters $\delta_\alpha^{E/F} \in \mathbb{R}$ encode the modification of tunneling rates and $\delta_\alpha^{E/F} = 0$ recovers the situation without feedback. The effective feedback generator reads in this case

$$\mathcal{L}_{\text{fb}}^I(\chi_\alpha) = \mathcal{L}_E(\chi_\alpha) \begin{pmatrix} 1 & 0 \\ 0 & 0 \end{pmatrix} + \mathcal{L}_F(\chi_\alpha) \begin{pmatrix} 0 & 0 \\ 0 & 1 \end{pmatrix}. \quad (3)$$

An extremal form of this feedback scheme would be to cut the left junction as soon as the SET is filled ($\delta_L^F \rightarrow -\infty$) and to cut the right junction when it is empty ($\delta_R^E \rightarrow -\infty$), which automatically implies unidirectional transport – independent of potential or temperature gradients. This effectively implements a feedback ratchet with two teeth – compare also Fig. 1 bottom right. However, in the idealized classical limit where the electrons are localized either on the left lead, the SET, or the right lead, this ratchet does not directly perform work. The resulting effective Liouvillian $\mathcal{L}_{\text{fb}}^I$ cannot generally be written in the form of Eq. (1) using modified tunneling rates $\tilde{\Gamma}_\alpha > 0$ and Fermi functions $f_\alpha \in (0, 1)$. One can check numerically [6] that the ensemble average of trajectories generated with stochastic Schrödinger equations coincide with the solution from Eq. (3).

In our *scheme IIa*, we act with an instantaneous control operation conditioned on whether an electron has jumped in (e^{κ_I}) or out (e^{κ_O}) of the system, such that $\kappa_I(\chi_L, \chi_R) = \sum_\alpha \delta_\alpha^I \mathcal{F}_\alpha(\chi_\alpha)$, and $\kappa_O(\chi_L, \chi_R) = \sum_\alpha \delta_\alpha^O \mathcal{F}_\alpha(\chi_\alpha)$, where $\delta_{R/L}^{I/O} \geq 0$ are dimensionless parameters roughly given by the product of pulse width and height of the time-dependent tunneling rates. The counting-field dependence arises from the simple fact that now – during the control operation – electrons may tunnel through the junctions (these tunneling events do not trigger further control operations): In fact, for infinitely strong feedback at one junction and zero feedback at the other junction (e.g. $\delta_L^I \rightarrow \infty$ and $\delta_R^I \rightarrow 0$) one obtains im-

mediate equilibration of the SET with the lead to which it is tunnel-coupled (e.g. $e^{\kappa_I(0,0)} \rho \rightarrow (1 - f_L, f_L)$ for all ρ). These tunneling events have to be taken into account when the complete statistics is required. Using from Eq. (2) the decomposition $\mathcal{F}_\alpha(\chi_\alpha) \equiv \mathcal{F}_\alpha^0 + \mathcal{F}_\alpha^+ e^{+i\chi_\alpha} + \mathcal{F}_\alpha^- e^{-i\chi_\alpha}$, the full effective feedback Liouvillian reads

$$\begin{aligned} \mathcal{L}_{\text{fb}}^{IIa}(\chi_\alpha) &= e^{\kappa_O(\chi_\alpha)} \mathcal{J}_O + e^{\kappa_I(\chi_\alpha)} \mathcal{J}_I + \sum_\alpha \Gamma_\alpha \mathcal{F}_\alpha^0, \quad (4) \\ \mathcal{J}_O &\equiv \sum_\alpha \Gamma_\alpha \mathcal{F}_\alpha^+ e^{+i\chi_\alpha}, \quad \mathcal{J}_I \equiv \sum_\alpha \Gamma_\alpha \mathcal{F}_\alpha^- e^{-i\chi_\alpha}, \end{aligned}$$

such that jumps in and out of the system are immediately followed by the respective control operation. In contrast to feedback schemes modifying the system Hamiltonian [7] it is no longer possible to simply shift counting fields by control operators. Solutions from Eq. (4) coincide with ensemble averages of the stochastic Schrödinger equation [6].

For an infinitely fast processing of the QPC trajectory, it would also be possible to recursively trigger further control operations when tunneling events take place during control. In our *scheme IIb* we restrict ourselves to the case that during the control operations only one junction admits tunneling at a time, i.e. $\delta_L^I = \delta_R^O = 0$. Then, we may also derive an effective feedback master equation for a recursive feedback scheme, where electrons tunneling during a control operation would induce further control operations – possibly ad infinitum (at infinite bias and infinite feedback strength). In this case, we may use the decompositions [6] $e^{\kappa_O(\chi_L)} \equiv \mathcal{P}^O(\chi_L) = \mathcal{P}_N^O + \mathcal{P}_O^O e^{+i\chi_L} + \mathcal{P}_I^O e^{-i\chi_L}$ and $e^{\kappa_I(\chi_R)} \equiv \mathcal{P}^I(\chi_R) = \mathcal{P}_N^I + \mathcal{P}_I^I e^{-i\chi_R} + \mathcal{P}_O^I e^{+i\chi_R}$ together with the evident relations $\mathcal{P}_O^O(\mathcal{F}_L^+ + \mathcal{F}_R^+) = \mathcal{P}_I^I(\mathcal{F}_L^- + \mathcal{F}_R^-) = \mathcal{P}_O^O \mathcal{P}_I^O = \mathcal{P}_I^I \mathcal{P}_O^O = \mathbf{0}$ (these effectively imply that during the control operations, the transport is unidirectional) to sum up the infinitely many terms as a von-Neumann operator series. Eventually [6], this results in the effective feedback Liouvillian

$$\begin{aligned} \mathcal{L}_{\text{fb}}^{IIb}(\chi_\alpha) &= \sum_\alpha \Gamma_\alpha \mathcal{F}_\alpha^0 \quad (5) \\ &+ (\mathcal{P}_N^O + e^{-i\chi_L} \mathcal{P}_N^I \mathcal{P}_I^O) \mathcal{W}(\mathcal{P}_O^I \mathcal{P}_I^O, \chi_\alpha) \mathcal{J}_O \\ &+ (\mathcal{P}_N^I + e^{+i\chi_R} \mathcal{P}_N^O \mathcal{P}_O^I) \mathcal{W}(\mathcal{P}_I^O \mathcal{P}_O^I, \chi_\alpha) \mathcal{J}_I \end{aligned}$$

with jump superoperators defined in Eq. (4) but now with the resolvent $\mathcal{W}(\mathcal{A}, \chi_R, \chi_L) \equiv [\mathbf{1} - \mathcal{A} e^{i(\chi_R - \chi_L)}]^{-1}$. Also for this scheme, mean occupation and statistics of tunneled particles may be compared with the stochastic Schrödinger equation [6].

Eqns. (3), (4), (5) yield the complete statistics for the current through the SET under the different feedback schemes: The generating function for its cumulants is in the long term given by the dominant (with $\lambda(0,0) = 0$) eigenvalue $\lambda(\chi_L, \chi_R)$ of the effective Liouvillians. In the idealized classical limit, none of the schemes performs

work on the system. However, quantum-mechanically the time-dependent modification of the tunneling rates changes the energy spectrum of the total Hamiltonian and thereby performs work [8].

Current We summarize the behavior of the current for finite feedback strengths at reverse infinite bias ($f_L = 0$, $f_R = 1$), zero bias ($f_L = f_R = f$), and infinite bias ($f_L = 1$, $f_R = 0$) for the different feedback schemes in table I. For finite temperatures (where $0 < f < 1$)

scheme	$V_{\text{bias}} \rightarrow -\infty$	$V_{\text{bias}} = 0$	$V_{\text{bias}} \rightarrow +\infty$
I	$-e^{-\delta_{\text{fb}}}/2$	$2f(1-f) \sinh(\delta_{\text{fb}})$	$e^{\delta_{\text{fb}}}/2$
IIa	$-1/2$	$f(1-f)(1 - e^{-\delta_{\text{fb}}})$	$1 - e^{-\delta_{\text{fb}}}/2$
IIb	$-1/2$	$\frac{f(1-f)(e^{\delta_{\text{fb}}}-1)}{2f(1-f)+e^{\delta_{\text{fb}}}[1-2f(1-f)]}$	$e^{\delta_{\text{fb}}}/2$

TABLE I: Values of the current (in units of $\Gamma_L = \Gamma_R = \Gamma$) under finite but symmetric feedback. The feedback parameters have been chosen as $\delta_L^F = \delta_R^E = -\delta_{\text{fb}}$ and $\delta_R^F = \delta_L^E = \delta_{\text{fb}}$ for scheme I and $\delta_R^I = \delta_L^O = \delta_{\text{fb}}$ as well as $\delta_L^I = \delta_R^O = 0$ for schemes IIa and IIb, respectively.

feedback may induce a current even at zero bias, such that the device acts as a MD shuffling electrons from one bath to another (here from left to right) using only the available information. This has to be contrasted with feedback ratchets [9] where the time-dependent ratchet potential performs work. The apparent divergence of the current in feedback scheme I for infinite bias and feedback strength is natural as the tunneling rates diverge likewise. For feedback scheme IIb however, we observe a genuine feedback catastrophe for large bias and large feedback strength leading to a divergent current: Control operations mutually trigger further control operations with vanishing halting probability, which leads to avalanche-like transport (in contrast to scheme I, the Fano factor also diverges in this region [6]). Naturally, there exists a parameter regime where the device transports electrons against an existing electrical or thermal gradient, where e.g. electrons are transported from left to right even though $f_L < f_R$, compare also Fig. 2. For scheme I, this effectively implements a Parrondo game (ratchet): Playing two losing strategies (tunneling with the bias) in an alternating manner may yield a winning strategy (tunneling against the bias) [10]. For our model, feedback is necessary to achieve such a current inversion: Without feedback, the long-term cumulant-generating function for the current obeys the analytic relation $\lambda(0, -\chi) = \lambda\left(0, +\chi - i \ln \left[\frac{(1-f_L)f_R}{f_L(1-f_R)}\right]\right)$, which when both leads are at the same temperature eventually leads to the fluctuation theorem [11–13] $\lim_{t \rightarrow \infty} \frac{P_n(t)}{P_{-n}(t)} = e^{+n\beta(\mu_L - \mu_R)}$. This implies that for a constant Liouvillian (1), the current $I = \lim_{t \rightarrow \infty} d/dt \sum_n n P_n(t)$ always flows from reservoirs with large chemical potential towards the reservoir with the smaller chemical potential. Also with open-loop feedback, where control operations are applied un-

conditionally (e.g., in a random or periodic manner), we find that the current will never flow against the electrothermal gradient – as long as no work is performed on the SET itself (i.e., the SET level ϵ remains unchanged) [6].

For scheme I we find that the Johnson-Nyquist relation normally relating noise with differential conductance at zero bias voltage (at similar temperatures left and right) is now shifted to the equilibrium voltage $V^* = (-\delta_L^E - \delta_R^F + \delta_R^E + \delta_L^F)/\beta$ at which the current vanishes $I(V^*) = 0$, i.e., more explicitly we have $S|_{V=V^*} = \frac{2}{\beta} \frac{dI}{dV}|_{V=V^*}$. We obtain a similarly simple modification of the fluctuation theorem for the electron counting statistics under feedback: The cumulant-generating function for the current obeys

$$\lambda^I(-\chi) = \lambda^I\left(+\chi - i \ln \left[\frac{(1-f_L)f_R}{f_L(1-f_R)} e^{\beta V^*}\right]\right), \quad (6)$$

which for both leads at the same temperature yields for the counting statistics $\lim_{t \rightarrow \infty} \frac{P_n(t)}{P_{-n}(t)} = e^{n\beta(\mu_L - \mu_R - V^*)}$. This formula directly demonstrates that the current may be directed against a potential gradient when the feedback parameters are adjusted accordingly.

For feedback schemes IIa and IIb, the equilibrium voltage V^* can be obtained numerically and depends on the baseline tunneling rates Γ_α .

Maximum Power at maximum Feedback For schemes IIa and IIb we may take $\delta_R^I = \delta_L^O \rightarrow \infty$ and $\delta_L^I = \delta_R^O = 0$ to obtain the maximum effect, but to bound the Liouvillian for scheme I we constrain ourselves to finite feedback strengths $\delta_L^E = \delta_R^F = +\delta_{\text{fb}}$ and $\delta_R^E = \delta_L^F = -\delta_{\text{fb}}$. The power $P = -IV$ generated by the MD can – when both leads are at the same temperature β be evaluated as $P\beta = -I\beta(\mu_L - \mu_R) = -I(f_L, f_R) \ln \left[\frac{f_L(1-f_R)}{f_R(1-f_L)}\right]$. The right hand side of this expression can for given Γ_L and Γ_R be numerically maximized with respect to the Fermi functions $f_{L/R} \in (0, 1)$ yielding the maximum power generated by the device, see table II. The maximum power generated with scheme I

scheme	$\Gamma_L = \Gamma_R = \Gamma$	$\Gamma_{\text{max}} \gg \Gamma_{\text{min}}$
IIa	$0.0841 \Gamma k_B T$	$0.1219 \Gamma_{\text{max}} k_B T$
IIb	$0.1892 \Gamma k_B T$	$0.1589 \Gamma_{\text{max}} k_B T$

TABLE II: Maximum power generated with the device for schemes IIa and IIb at maximum unidirectional feedback for symmetric and highly asymmetric tunneling rates.

is unbounded (as the Liouvillian) and asymptotically approaches $0.2785 \Gamma e^{\delta_{\text{fb}}} k_B T$ for symmetric tunneling rates. Even under idealized conditions, the associated work performed by the MD has to be contrasted with the heat dissipated when the QPC trajectory data-points are deleted (Landauer principle). To perform the continuous monitoring of the SET it is important that the QPC sampling rate $\Delta\tau^{-1}$ is greater than the maximum tunneling rate

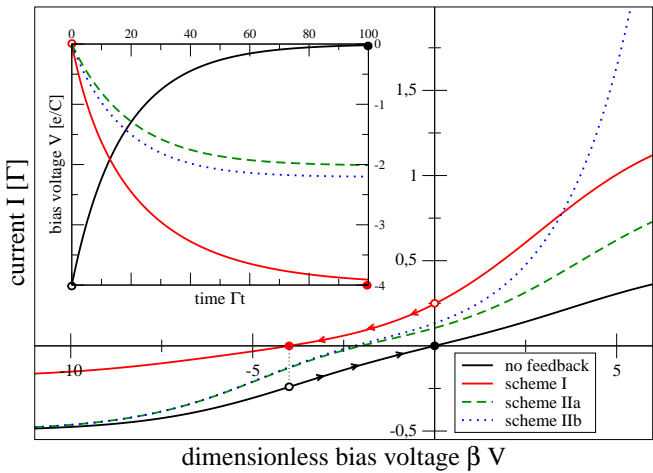


FIG. 2: Current-voltage characteristics under feedback strength $\delta_L^E = \delta_R^F = -\delta_R^E = -\delta_L^F = 1$ in scheme I (red solid curve) and maximum feedback in schemes IIa and IIb for symmetric tunneling rates $\Gamma_L = \Gamma = \Gamma_R$ and $\beta\epsilon = 2$. The current may point in the other direction than the voltage leading to a positive power generated by the device. The inset (for $\beta e/C = 1$) shows the mean-field evolution of the voltage from an initial value (empty circles) to the stable fixed points (filled circle) for symmetric capacitances of the two conductors.

$\Delta\tau < \Gamma_{\max}^{-1}$ (or $\Delta t \leq \Gamma_{\max} e^{-\delta^{\text{fb}}}$ for scheme I). This implies that the maximum work per current measurement $W = P_{\max}\Delta\tau$ is always smaller than the dissipated Landauer heat by the MD, such that the results are compatible with the second law.

Feedback Charging Effects Small leads of finite capacitances will usually be driven out of equilibrium due to transport. Additional larger reservoirs at thermal equilibrium may however immediately re-enforce equilibrium in the leads solely by scattering interactions (without electron tunneling). We may phenomenologically include this effect by making the chemical potentials dependent on the number of tunneled particles: Starting at equilibrium, the difference V in chemical potentials between the two leads is classically simply proportional to the number of tunneled particles $V = en/C$, where C denotes the total capacitance (similar relations hold for left and right chemical potentials in case of asymmetric capacitances [14]). We may numerically solve the resulting mean-field nonlinear [6] differential equation $\dot{V} = e/C \langle \dot{n}(t) \rangle = eI(V)/C$ to obtain the timescale after which we have sufficiently approached the flow equilibrium ($I(V^*) = 0$), compare the inset in Fig. 2. After this time, feedback may be stopped and the current will reverse its direction (black trajectory). With the QPC already in place, it appears reasonable to use it as a detector to clearly discriminate the resulting initial fluctuations from equilibrium ones. This scheme works as an accumulator undergoing charging (feedback) and discharging (no-feedback) cycles, where the total stored

energy is given by $W = C(V^*)^2/(2e)$.

Experimental implementation With gate voltages, the height of the tunneling barriers may be adjusted such that the timescale on which electrons tunnel through the QPC can be tuned from ms [15] to seconds and even hours. For periodically varying gate voltages, the frequency corresponds with 100 MHz to switching times five orders of magnitude smaller in recent electron pumping experiments [16, 17]. The bandwidth of typical experimental QPC detector devices has been reported in the range of 40 kHz, with sufficiently larger current sampling frequencies of 100 kHz [18]. The experimental challenge therefore clearly lies in the necessity of strongly modifying the tunneling rates without performing work on the system (changing the SET level). With gate electrodes of sizes below 100 nm [17] it should be possible to keep the energy level of the SET (size about 300 nm [15]) approximately constant.

Summary To conclude, we have compared several closed-loop feedback schemes implementing a Maxwell demon by means of an effective feedback master equation. All schemes are capable of generating a current against a moderate bias and may for finite-size leads be used to charge a feedback battery. Schemes I and IIa (at finite feedback strength) should be implementable with present-day technology, whereas the feedback recursion depth appears to be currently limited by the QPC sampling frequency.

Financial support by the DFG (grant SCHA 1646/2-1, SFB 910) and stimulating discussions with T. Novotný are gratefully acknowledged.

* Electronic address: gernot.schaller@tu-berlin.de

- [1] K. Maruyama, F. Nori, and V. Vedral, *Rev. Mod. Phys.* **81**, 1 (2009).
- [2] S. Datta, e-print arXiv:0704.1623v1.
- [3] M. Esposito and K. Lindenberg and C. Van den Broeck, *Europhys. Lett.* **85**, 60010 (2009).
- [4] Y. V. Nazarov, *Quantum Noise in Mesoscopic Physics*, Kluwer Academic, Dordrecht (2003).
- [5] H.-P. Breuer and F. Petruccione, *The Theory of Open Quantum Systems*, Oxford University Press (2002).
- [6] See the online supplementary material.
- [7] H. M. Wiseman and G. J. Milburn, *Quantum Measurement and Control*, Cambridge University Press (2010).
- [8] S. W. Kim *et al.* *Phys. Rev. Lett.* **106**, 070401 (2011).
- [9] F. J. Cao, M. Feito, and H. Touchette, *Physica A* **388**, 113 (2009).
- [10] G. P. Harmer and D. Abbott, *Nature* **402**, 864 (1999).
- [11] M. Esposito and U. Harbola and S. Mukamel, *Rev. Mod. Phys.* **81**, 1665 (2009).
- [12] K. Saito and Y. Utsumi, *Phys. Rev. B* **78**, 115429 (2008).
- [13] Y. Utsumi and K. Saito, *Phys. Rev. B* **79**, 235311 (2009).
- [14] J. D. Jackson, *Classical Electrodynamics*, John Wiley and Sons, New York (1998).
- [15] S. Gustavsson *et al.*, *Phys. Rev. Lett.* **96**, 076605 (2006).
- [16] M. D. Blumenthal *et al.*, *Nature Physics* **3**, 343 (2007).

[17] N. Maire *et al.*, Appl. Phys. Lett. **92**, 082112 (2008).

[18] C. Flindt *et al.* PNAS **106**, 10116 (2009).

Appendix A: Effective master equation for scheme I

Assuming that the dot is empty at time t , i.e., $\rho(t) = (1, 0)$, its no-measurement time evolution under feedback scheme I will be governed by $\rho(t + \Delta t) = e^{\mathcal{L}_E(\chi_L, \chi_R)\Delta t}\rho(t)$, whereas for an initially filled dot $\rho(t) = (0, 1)$, we will have the evolution $\rho(t + \Delta t) = e^{\mathcal{L}_F(\chi_L, \chi_R)\Delta t}\rho(t)$. Using projection superoperators on the empty and filled dot states, respectively, both cases can be incorporated into a single equation

$$\rho(t + \Delta t) = \left[e^{\mathcal{L}_E(\chi_L, \chi_R)\Delta t} \begin{pmatrix} 1 & 0 \\ 0 & 0 \end{pmatrix} + e^{\mathcal{L}_F(\chi_L, \chi_R)\Delta t} \begin{pmatrix} 0 & 0 \\ 0 & 1 \end{pmatrix} \right] \rho(t). \quad (7)$$

Expanding the propagators for small Δt , using that the projection operators add up to the identity, and solving for the finite-difference $[\rho(t + \Delta t) - \rho(t)]/\Delta t$ yields the effective feedback Liouvillian Eq. (3). The switching between the different propagators is assumed to be instantaneous, such that during the switching time, no particles may tunnel. Therefore, the original counting fields may simply be kept, and effectively, the Liouvillian (3) has the first column from \mathcal{L}_E and the second column from \mathcal{L}_F

$$\mathcal{L}_{\text{fb}}^I(\chi_L, \chi_R) = \begin{pmatrix} -\Gamma_L e^{\delta_L^E} f_L - \Gamma_R e^{\delta_R^E} f_R & +\Gamma_L e^{\delta_L^F} e^{+i\chi_L} (1 - f_L) + \Gamma_R e^{\delta_R^F} e^{+i\chi_R} (1 - f_R) \\ +\Gamma_L e^{\delta_L^E} e^{-i\chi_L} f_L + \Gamma_R e^{\delta_R^E} e^{-i\chi_R} f_R & -\Gamma_L e^{\delta_L^F} (1 - f_L) - \Gamma_R e^{\delta_R^F} (1 - f_R) \end{pmatrix}, \quad (8)$$

which explicitly breaks detailed balance.

A single trajectory for this feedback scheme may be easily generated as follows: Assuming that e.g. the dot is initially filled, the probability that during a small timestep Δt the electron jumps out to the left is given by $P_{\text{left}}^F(\Delta t) = \Delta t \Gamma_L e^{\delta_L^F} (1 - f_L)$, whereas the probability to jump out to the right reads $P_{\text{right}}^F(\Delta t) = \Delta t \Gamma_R e^{\delta_R^F} (1 - f_R)$. The probabilities for electrons jumping from left or right lead into an initially empty dot are obtained similarly and read $P_{\text{left}}^E(\Delta t) = \Delta t \Gamma_L e^{\delta_L^E} f_L$ and $P_{\text{right}}^E(\Delta t) = \Delta t \Gamma_R e^{\delta_R^E} f_R$. Using a random number generator, one may with sufficiently small timesteps (such that the probabilities are significantly smaller than one) generate single trajectories for the dot occupation n , the number of tunneled particles to the left lead n_L , and the number of particles tunneled to the right lead n_R . The ensemble average of many such trajectories may now be compared with the analytic solution of the effective feedback master equation (3), see Fig. 3. It follows that for sufficiently many trajectories the same average observables will be obtained as with the effective feedback master equation.

Appendix B: Effective master equation for scheme IIa

When ultrafast control operations are only to be applied whenever an electron jumps into or out of the dot, the derivation of an effective master equation is a bit more involved. We start from the inverse Fourier transform of the evolution generated by Eq. (2)

$$\rho^{(n_L, n_R)}(t + \Delta t) = \left[\frac{1}{(2\pi)^2} \int_{-\pi}^{+\pi} d\chi_L \int_{-\pi}^{+\pi} d\chi_R e^{\mathcal{L}(\chi_L, \chi_R)\Delta t - in_L \chi_L - in_R \chi_R} \right] \rho(t), \quad (9)$$

where $\rho(t)$ denotes the unconditional dot density matrix at time t , and $n_{L/R}$ the number of electrons that have tunneled to left/right reservoirs during the timestep Δt . For small Δt it suffices to consider single-particle jumps only. Expanding the propagator for small Δt and using the orthonormality relation $\int_{-\pi}^{+\pi} e^{i(n-m)\chi} d\chi = 2\pi \delta_{nm}$ we obtain the conditional evolution equations

$$\begin{aligned} \rho^{(0,0)}(t + \Delta t) &= [\mathbf{1} + \Delta t (\mathcal{F}_L^0 + \mathcal{F}_R^0)] \rho(t), \\ \rho^{(+1,0)}(t + \Delta t) &= \Delta t \mathcal{F}_L^+ \rho(t), & \rho^{(-1,0)}(t + \Delta t) &= \Delta t \mathcal{F}_L^- \rho(t), \\ \rho^{(0,+1)}(t + \Delta t) &= \Delta t \mathcal{F}_R^+ \rho(t), & \rho^{(0,-1)}(t + \Delta t) &= \Delta t \mathcal{F}_R^- \rho(t), \end{aligned} \quad (10)$$

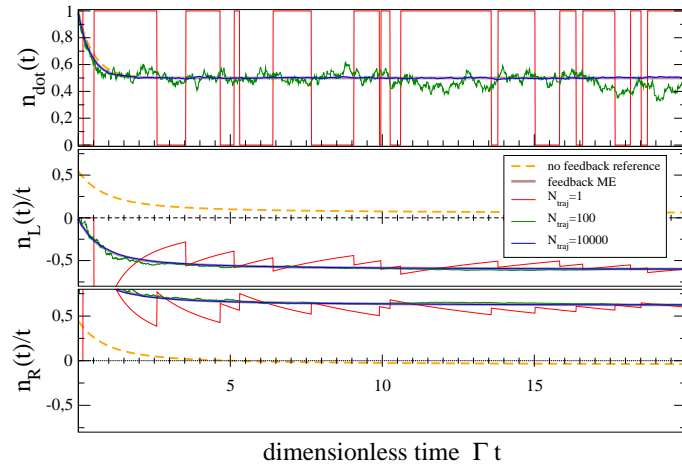


FIG. 3: Comparison of a single (red, same realization in all panels) and the average of 100 (green) and 10000 (blue) trajectories with the solution from the effective feedback master equation (3) for the dot occupation (top), the number of particles on the left (middle), and the number of particles on the right (bottom). The average of the trajectories converges to the effective feedback master equation result. The reference curve without feedback (dashed orange) may be obtained from Eq. (2) or by using vanishing feedback parameters and demonstrates that the direction of the current may actually be reversed via sufficiently strong feedback. Parameters: $\Gamma_L = \Gamma_R \equiv \Gamma$, $f_L = 0.45$, $f_R = 0.55$, $\delta_L^E = \delta_R^E = 1.0$, $\delta_R^E = \delta_L^E = -10.0$, and $\Gamma\Delta t = 0.01$.

and the respective probabilities are simply given by the trace of these operators. To derive a master equation accounting for the average evolution of observables without feedback one may simply compute the weighted average $\bar{\rho}(t + \Delta t) = \rho^{(0,0)} + \rho^{(+1,0)} + \rho^{(-1,0)} + \rho^{(0,+1)} + \rho^{(0,-1)}$, which would after solving for the finite difference scheme $(\bar{\rho}(t + \Delta t) - \rho(t))/\Delta t$ yield the original Liouvillian in Eq. (1). In contrast, with δ -kick feedback operations e.g.

$$\kappa_I = \int_t^{t+\tau} \mathcal{L}_I^{\text{control}}(t') dt' = \delta_L^I \mathcal{F}_L(0) + \delta_R^I \mathcal{F}_R(0) = \begin{pmatrix} -\delta_L^I f_L - \delta_R^I f_R & +\delta_L^I (1 - f_L) + \delta_R^I (1 - f_R) \\ +\delta_L^I f_L + \delta_R^I f_R & -\delta_L^I (1 - f_L) - \delta_R^I (1 - f_R) \end{pmatrix} \quad (11)$$

and similarly for κ_O , where $\delta_L^{I/O}$ are dimensionless feedback parameters characterizing the product of pulse height and width, we have to perform the average after applying the matching feedback operation [in (I) or out (O)]

$$\bar{\rho}(t + \Delta t) = \rho^{(0,0)} + e^{\kappa_O} \rho^{(+1,0)} + e^{\kappa_I} \rho^{(-1,0)} + e^{\kappa_O} \rho^{(0,+1)} + e^{\kappa_I} \rho^{(0,-1)}. \quad (12)$$

After converting this into a finite-difference equation we would obtain the generator in Eq. (4) without counting fields. Now it is obvious and essential that during the control operations, electrons may tunnel through the junctions, such that counting fields may be re-introduced via a conditional master equation. Finally, this yields the form of Eq. (4).

For the trajectories we constrain ourselves to opening only one junction at a time for all control operations, e.g. $\delta_L^I = \delta_R^O = 0$ in order to avoid an unbounded number of particles tunneling during control. It is straightforward to compute the trajectories as described before, see Fig. 4. The computed trajectories do well converge to the results of the effective feedback master equation. The scheme is non-recursive, i.e., electrons tunneling during control operations do not trigger a further control operation.

Appendix C: Effective master equation for scheme IIb

In order to resum the control operations when applied recursively, it is essential that only one junction is opened at a time, formally expressed by choosing $\delta_L^I = \delta_R^O = 0$. This implies that once a control operation has been triggered initially, the transport becomes unidirectional, which allows for a simple analytic resummation. We note that in this

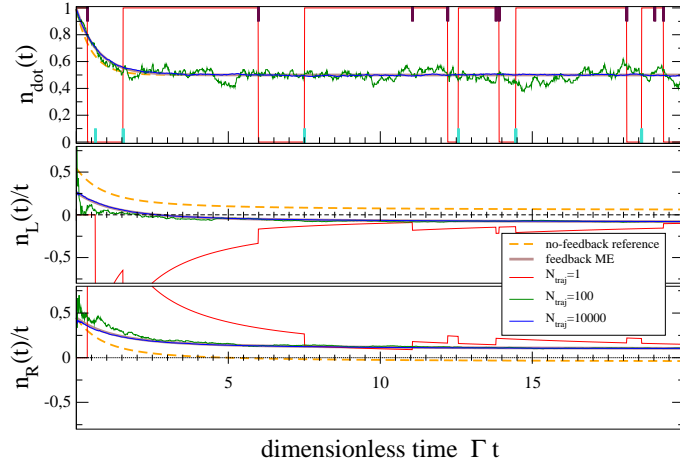


FIG. 4: Comparison of a single (red) and the average of 100 (green) and 10000 (blue) trajectories with the solution from the effective feedback master equation (4) for the dot occupation (top), the number of particles on the left (middle), and the number of particles on the right (bottom). The average of the trajectories converges to the effective feedback master equation result. The single trajectory (red) does not track multiple electron jumps when they have no net effect. Therefore, control operations (bold kinks in top graph) are not always correlated with a net change in the occupation or the particle number left and right. Color coding and parameters are as in Fig. 3 where applicable. Feedback parameters were chosen as $\delta_L^I = \delta_R^O = 0$ and $\delta_R^I = \delta_L^O = 1.0$.

case we have the simple decomposition

$$e^{\kappa_O(\chi_L)} \equiv P^O = P_N^O + P_O^O + P_I^O = \begin{pmatrix} 1 - (1 - e^{-\delta_L^O})f_L & e^{+i\chi_L}(1 - e^{-\delta_L^O})(1 - f_L) \\ e^{-i\chi_L}(1 - e^{-\delta_L^O})f_L & 1 - (1 - e^{-\delta_L^O})(1 - f_L) \end{pmatrix},$$

$$e^{\kappa_I(\chi_R)} \equiv P^I = P_N^I + P_O^I + P_I^I = \begin{pmatrix} 1 - (1 - e^{-\delta_R^I})f_R & e^{+i\chi_R}(1 - e^{-\delta_R^I})(1 - f_R) \\ e^{-i\chi_R}(1 - e^{-\delta_R^I})f_R & 1 - (1 - e^{-\delta_R^I})(1 - f_R) \end{pmatrix}, \quad (13)$$

where we have $P_N^{O/I} = \mathcal{P}_N^{O/I}$, $P_O^O = \mathcal{P}_O^O e^{+i\chi_L}$, $P_I^O = \mathcal{P}_I^O e^{-i\chi_L}$, $P_I^I = \mathcal{P}_I^I e^{-i\chi_R}$, and $P_O^I = \mathcal{P}_O^I e^{+i\chi_R}$ and where the lower indices mark the parts responsible for no particle change (N), a particle jumping out of the system (O, possible for κ_I only to the right), and a particle jumping into the system (I, possible for κ_O only from the left). The fact that out of an empty system, no particle may jump out and vice versa for a filled SET system no further particle may jump in is formally reflected in the relations $P_O^O \mathcal{L}_{0+} = P_O^O \mathcal{L}_{+0} = \mathbf{0}$ and $P_I^I \mathcal{L}_{-0} = P_I^I \mathcal{L}_{0-} = \mathbf{0}$ as well as $P_I^I P_O^I = P_O^O P_I^O = \mathbf{0}$. Therefore, to generalize the first-order feedback scheme IIa

$$\mathcal{L}_{\text{fb}}^{(1)} = \Gamma_L \mathcal{F}_L^0 + \Gamma_R \mathcal{F}_R^0 + (P_N^O + P_I^O)(e^{+i\chi_L} \mathcal{F}_L^+ + e^{+i\chi_R} \mathcal{F}_R^+) + (P_N^I + P_O^I)(e^{-i\chi_L} \mathcal{F}_L^- + e^{-i\chi_R} \mathcal{F}_R^-) \quad (14)$$

to a recursive feedback scheme (IIb) with a potentially infinite recursion depth requires to recursively follow the replacement scheme

$$\begin{aligned} P_N^O \mathcal{A} &\rightarrow P_N^O \mathcal{A}, \\ P_I^O \mathcal{A} &\rightarrow (P_N^I + P_O^I) P_I^O \mathcal{A}, \\ P_N^I \mathcal{A} &\rightarrow P_N^I \mathcal{A}, \\ P_O^I \mathcal{A} &\rightarrow (P_N^O + P_I^O) P_O^I \mathcal{A} \end{aligned} \quad (15)$$

for arbitrary operators \mathcal{A} , which eventually leads to

$$\begin{aligned} \mathcal{L}_{\text{fb}}^{(\infty)} &= \Gamma_L \mathcal{F}_L^0 + \Gamma_R \mathcal{F}_R^0 \\ &+ (P_N^O + P_N^I P_I^O) \left[\sum_{n=0}^{\infty} (P_O^I P_I^O)^n \right] (e^{+i\chi_L} \mathcal{F}_L^+ + e^{+i\chi_R} \mathcal{F}_R^+) \\ &+ (P_N^I + P_N^O P_O^I) \left[\sum_{n=0}^{\infty} (P_I^O P_O^I)^n \right] (e^{-i\chi_L} \mathcal{F}_L^- + e^{-i\chi_R} \mathcal{F}_R^-). \end{aligned} \quad (16)$$

After summing the von-Neumann operator series and using $\mathcal{P}_N^O = P_N^O$, $\mathcal{P}_N^I = P_N^I$, $P_O^I = \mathcal{P}_O^I e^{+i\chi_R}$, and $P_I^O = \mathcal{P}_I^O e^{-i\chi_L}$ we finally obtain Eq. (5).

Similarly, we may recursively construct the trajectories numerically, see Fig. 5. The tunneling during mutually

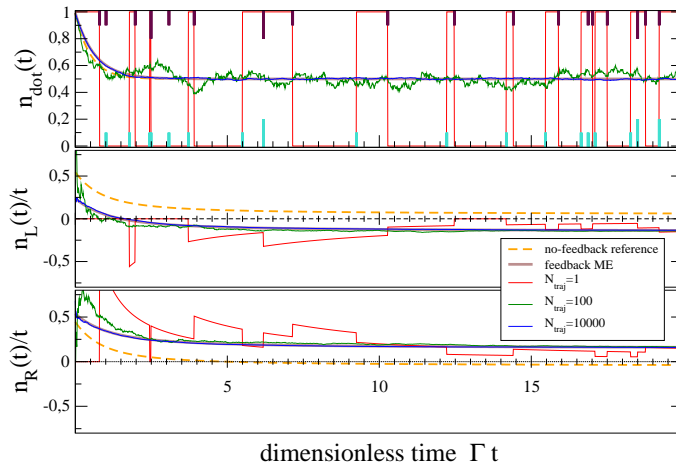


FIG. 5: Comparison of a single (red) and the average of 100 (green) and 10000 (blue) trajectories with the solution from the effective feedback master equation (5) for the dot occupation (top), the number of particles on the left (middle), and the number of particles on the right (bottom). The average of the trajectories converges to the effective feedback master equation result. Electrons jumping during control operations may now recursively trigger further control operations – marked by the height of the bold kinks in the top graph. Color coding and parameters are as in Fig. 4.

calling control operations is only stopped after no particle tunnels. At infinite bias and infinite feedback strength, the corresponding halting probability vanishes, which leads to a feedback catastrophe. Precursors of this are already observed at finite feedback strength and infinite bias in the large current and Fano factor – compare right columns in tables I and III – or at infinite feedback strength and finite bias in the current – compare the dotted curve in Fig. 2.

Appendix D: Unconditional control leads to transport with the bias

This statement is mainly based on detailed balance, where we assume without loss of generality $f_L < f_R$.

By evaluating the stationary states $\bar{\rho} = (1 - \bar{n}^{\text{SET}}, \bar{n}^{\text{SET}})^T$ of Liouvillians \mathcal{L} , \mathcal{L}_E , and \mathcal{L}_F one can see that their stationary occupation \bar{n}^{SET} is within the transport corridor $f_L \leq \bar{n}^{\text{SET}} \leq f_R$ with the actual position depending on the respective tunneling rates. With any state within the transport corridor as initial condition one can show that the propagators $\mathcal{P} \in \{e^{\mathcal{L}\Delta t}, e^{\mathcal{L}_E\Delta t}, e^{\mathcal{L}_R\Delta t}, e^{\kappa_I}, e^{\kappa_O}\}$ again map to occupations $\rho_{i+1} = (1 - n_{i+1}^{\text{SET}}, n_{i+1}^{\text{SET}})^T = \mathcal{P}(1 - n_i^{\text{SET}}, n_i^{\text{SET}})^T = \mathcal{P}\rho_i$ within the corridor, i.e. for all $f_L \leq n_i^{\text{SET}} \leq f_R$ we have $f_L \leq n_{i+1}^{\text{SET}} \leq f_R$. This implies that once any unconditional iterative control scheme has entered the transport corridor (large times), it will not be able to leave it again, regardless of the timesteps Δt , control parameters, baseline tunneling rates, and the order of the operations. In contrast, with the conditioned feedback scheme one is always outside this corridor with $n_i^{\text{SET}} \in \{0, 1\}$. With inserting counting fields at e.g. the right junction $\mathcal{P} \rightarrow \mathcal{P}(\chi_R)$ one may now calculate the mean particle number tunneling during an iteration step

$$\Delta n_i = (-i)\partial_{\chi_R} \text{Tr} \{ \mathcal{P}(\chi_R)(1 - n_i^{\text{SET}}, n_i^{\text{SET}})^T \} \Big|_{\chi_R \rightarrow 0}, \quad (17)$$

when the initial state is within the transport corridor ($f_L \leq n_i^{\text{SET}} \leq f_R$). The outcome is that in this case the electron current always points from right to left when $f_L < f_R$, i.e. for similar temperatures with the bias.

Note also that for unconditional switching between the Liouvillians (scheme I), this is not a Parrondo game anymore, since a third possibility of game outcome (no tunneling event at all) is included.

Appendix E: Comparison of Fano Factors

We summarize the Fano factor $F = S/|I|$ given by the ratio of noise and current for finite feedback strength in Table III. Divergence of the Fano factor for scheme IIb at infinite feedback strength demonstrates the feedback

scheme	$V_{\text{bias}} \rightarrow -\infty$	$V_{\text{bias}} = 0$	$V_{\text{bias}} \rightarrow +\infty$
I	1/2	$\coth(\delta_{\text{fb}})/2 + (1-2f)^2 \tanh(\delta_{\text{fb}})/2$	1/2
IIa	1/2	$\frac{2f(1-f) + \cosh(\delta_{\text{fb}})[1-2f(1-f)] + \sinh(\delta_{\text{fb}})}{(1-2f)^2 [\cosh(\delta_{\text{fb}}) - 1] + \sinh(\delta_{\text{fb}})}$	$\frac{4-3e^{-\delta_{\text{fb}}}}{4-2e^{-\delta_{\text{fb}}}}$
IIb	1/2	$\frac{2e^{2\delta_{\text{fb}}} - e^{\delta_{\text{fb}}} + 1}{e^{2\delta_{\text{fb}}} - 1}$	$e^{\delta_{\text{fb}}} - 1/2$

TABLE III: Values of the Fano factor (assuming $\delta_{\text{fb}} \geq 0$) with the same parameters as in table I, the zero-bias Fano factor for scheme IIb has been evaluated for $f = 1/2$ only for brevity.

catastrophy. Also, at zero feedback the Fano factor should diverge at zero bias as this is the point where conventionally the current would vanish.

Appendix F: Nonlinear Current-Voltage Characteristics

The stationary current (e.g. at the right junction) may either be calculated from the cumulant-generating function or via the relation $I = (-i)\text{Tr} \left\{ \partial_{\chi_R} \mathcal{L}(\chi_L, \chi_R) \big|_{0,0} \bar{\rho} \right\}$, where $\mathcal{L}(0,0)\bar{\rho} = \mathbf{0}$ and reads for scheme I

$$I_{\text{fb}}^I = \frac{\Gamma_L \Gamma_R \left[e^{\delta_L^E + \delta_R^E} f_L (1 - f_R) - e^{\delta_L^E + \delta_R^E} (1 - f_L) f_R \right]}{\Gamma_L e^{\delta_L^E} (1 - f_L) + \Gamma_R e^{\delta_R^E} (1 - f_R) + \Gamma_L e^{\delta_L^E} f_L + \Gamma_R e^{\delta_R^E} f_R}, \quad (18)$$

where insertion of the Fermi functions $f_\alpha = [e^{\beta_\alpha(\epsilon - \mu_\alpha)} + 1]^{-1}$ at similar temperatures $\beta_L = \beta_R = \beta$ and symmetric chemical potentials $\mu_L = +V/2$ and $\mu_R = -V/2$ yields the full nonlinear current-voltage characteristics displayed in Fig. 2.

For feedback schemes IIa and IIb the expressions become a bit lengthy, such that we only give the maximum feedback limit $\delta_L^I = \delta_R^O = 0$ and $\delta_R^I = \delta_L^O \rightarrow \infty$ for the current

$$\begin{aligned} I_{\text{fb}}^{IIa} &= \frac{f_L(1-f_R) [\Gamma_L^2(1-f_L)^2 + \Gamma_R^2 f_R^2] + \Gamma_L \Gamma_R [f_L - f_L^2 - f_R^2 - f_L f_R - 2f_L^2 f_R^2 + 2f_L f_R (f_L + f_R)]}{\Gamma_L [1 - f_L(1 - f_L + 1 - f_R)] + \Gamma_R [1 - (1 - f_R)(f_L + f_R)]}, \\ I_{\text{fb}}^{IIb} &= \frac{\Gamma_L^2 f_L(1-f_L)(1-f_R) + \Gamma_R^2 f_L f_R(1-f_R) + \Gamma_L \Gamma_R [f_L - f_R^2 - f_L^2 f_R + f_L f_R^2]}{\Gamma_L [1 - f_L(1 - f_L + 1 - f_R)] + \Gamma_R [1 - (1 - f_R)(f_L + f_R)]}. \end{aligned} \quad (19)$$

Again, insertion of the Fermi functions at similar temperatures and symmetric chemical potentials yields the nonlinear current-voltage characteristics in Fig. 2.